Molecular Biology of the Cell
Vol. 12, 3933–3946, December 2001

Dynamic Behavior of Microtubules during Dynein-dependent Nuclear Migrations of Meiotic Prophase in Fission Yeast

Ayumu Yamamoto,*†‡ Chihiro Tsutsumi1,† Hiroaki Kojima,§ Kazuhiro Oiwa,§ and Yasushi Hiraoka*†

*Cell Biology Group, †CREST Research Project, and §Protein Biophysics Group, Kansai Advanced Research Center, Communications Research Laboratory, Kobe 651-2492, Japan

Submitted April 13, 2001; Revised August 24, 2001; Accepted September 20, 2001
Monitoring Editor: J. Richard McIntosh

During meiotic prophase in fission yeast, the nucleus migrates back and forth between the two ends of the cell, led by the spindle pole body (SPB). This nuclear oscillation is dependent on astral microtubules radiating from the SPB and a microtubule motor, cytoplasmic dynein. Here we have examined the dynamic behavior of astral microtubules labeled with the green fluorescent protein during meiotic prophase with the use of optical sectioning microscopy. During nuclear migrations, the SPB mostly follows the microtubules that extend toward the cell cortex. SPB migrations start when these microtubules interact with the cortex and stop when they disappear, suggesting that these microtubules drive nuclear migrations. The microtubules that are followed by the SPB often slide along the cortex and are shortened by disassembly at their ends proximal to the cortex. In dynein-mutant cells, where nuclear oscillations are absent, the SPB never migrates by following microtubules, and microtubule assembly/disassembly dynamics is significantly altered. Based on these observations, together with the frequent accumulation of dynein at a cortical site where the directing microtubules interact, we propose a model in which dynein drives nuclear oscillation by mediating cortical microtubule interactions and regulating the dynamics of microtubule disassembly at the cortex.

INTRODUCTION

Cytoplasmic dynein is a complex of proteins that moves along microtubules toward their minus (slow-growing) ends (reviewed by Holzbaur and Vallee, 1994). It is involved in many biological activities. Recent studies have shown that dynein drives nuclear or spindle migrations in a variety of organisms, including fungi, slime molds, worms, and probably mammals (Eshel *et al.*, 1993; Li *et al.*, 1993; Plamann *et al.*, 1994; Xiang *et al.*, 1994, 1995; Yeh *et al.*, 1995; Inoue *et al.*, 1998; Gönczy *et al.*, 1999; Koonce *et al.*, 1999; Yamamoto *et al.*, 1999; reviewed by Reinsch and Gönczy, 1998 Karki and Holzbaur, 1999; Morris, 2000). Migration of the nucleus or spindle is generally driven by the interaction of astral microtubules with the cell cortex (Hyman and White, 1987; Hymann, 1989; Palmer *et al.*, 1992; Reinsch and Karsenti, 1994; Svoboda t al., 1995; Ding *et al.*, 1998; Neujahr *et al.*, 1998); this interaction is thought to be dependent on dynein (Carminati and Stearns, 1997; Gönczy *et al.*, 1999; Koonce *et al.*, 1999; Yamamoto *et al.*, 1999; Adames and Cooper, 2000; Xiang *et al.*, 2000). Dynein is also required for the proper dynamics of astral microtubules (Carminati and Stearns, 1997; Koonce *et al.*, 1999; Adames and Cooper, 2000; Han *et al.*, 2001). Despite this accumulating knowledge about roles of dynein, how dynein actually drives nuclear or spindle migration via microtubules remains largely unclear.

In the fission yeast, *Schizosaccharomyces pombe*, striking dynein-dependent nuclear migrations are observed during meiotic prophase. The nucleus becomes elongated and migrates back and forth between the two ends of the cell, led by the spindle pole body (SPB; the centrosome equivalent in fungi; Chikashige *et al.*, 1994). During this nuclear oscillation, the telomeres are clustered near the SPB and homologous chromosomes are aligned (Chikashige *et al.*, 1994; Niwa *et al.*, 2000). It has been proposed that the nuclear oscillation facilitates pairing of homologous chromosomes by aligning the chromosomes from the telomeres and promoting contact of homologous loci (Chikashige *et al.*, 1994; Kohli, 1994; Hiraoka, 1998; Yamamoto *et al.*, 1999; Yamamoto and Hiraoka, 2001). This proposition was supported by reductions in the frequencies of both recombination and colocalization of ho-

‡ Corresponding author. E-mail address: ayumu@crl.go.jp.
Abbreviations used: DHC, dynein heavy chain; GFP, green fluorescent protein; SPB, spindle pole body.

mologous loci in mutant cells in which the nuclear oscillation is abolished (Yamamoto *et al.*, 1999).

Nuclear oscillation in *S. pombe* is driven by astral microtubules (Svoboda *et al.*, 1995; Ding *et al.*, 1998) and cytoplasmic dynein (Yamamoto *et al.*, 1999). During nuclear oscillation, astral microtubules extend both forward and rearward from the SPB and interact with the cell cortex. Dynein heavy chain (DHC), a major component of cytoplasmic dynein, is localized on the microtubules and SPB. It also frequently accumulates at a site where forward-extending microtubules interact with the cortex and the nucleus migrates toward this site. Elimination of either microtubules or DHC abolishes nuclear oscillation.

It has been speculated that nuclear oscillations are driven by either a pulling force generated by the forward-extending microtubules or a pushing force generated by the rearward-extending ones, or a combination of both (Svoboda *et al.*, 1995; Ding *et al.*, 1998). Because microtubules are likely oriented with their minus ends proximal to the SPB, dynein immobilized at the cell cortex could generate a pulling force by walking along forward-extending microtubules (Yamamoto *et al.*, 1999; Yamamoto and Hiraoka, 2001). Alternatively, dynein localized at the SPB could generate a pushing force by moving along rearward-extending microtubules. The mechanism of nuclear oscillation remains mostly unknown.

To understand how dynein drives nuclear oscillation via astral microtubules, it is essential to study the relationship between microtubule behavior and nuclear migrations in detail. In this study, we have examined the dynamic behavior of astral microtubules labeled with green fluorescent protein (GFP) in wild-type and dynein-mutant cells with the use of optical sectioning microscopy. We have also examined the behavior of GFP-tagged DHC during nuclear oscillation. Based on our observations, we discuss how dynein may generate a force and drive meiotic nuclear oscillation in fission yeast.

MATERIALS AND METHODS

Strains and Media

The strains used in this study are a wild-type strain, CRL152 (h^{90} *leu1 lys1 ura4*), a dynein-mutant strain, CRL1521 (h^{90} *leu1 lys1 ura4 dhc1-d2*), and a strain containing the *dhc1*-GFP fusion gene, CRL1526 (h^{90} *leu1 lys1 ura4 dhc1::GFP-LEU2*; Yamamoto *et al.*, 1999). Media were prepared as described by Moreno *et al.* (1991), except that YE medium containing 75 mg/ml adenine sulfate (YEA medium) was used for routine growth of cells. Genetical techniques used in this study are described by Moreno *et al.* (1991).

Cell Preparation

Microtubule behavior was observed by expressing a GFP-alpha-tubulin fusion in homothalic haploid cells (strain CRL152 or CRL1521). Cells were transformed with a multicopy plasmid, pDQ105 (Ding *et al.*, 1998), which expresses the GFP-alpha-tubulin under the *nmt1* promoter (Maundrell, 1993). These cells were grown on solid YEA medium at 33°C for ~24 h. They were transferred on solid ME medium and incubated at 26°C for an additional 12–14 h. GFP-tagged DHC was observed in homothalic haploid strain CRL1526 as described for GFP-alpha-tubulin. Cells with opposite mating types conjugate with each other to become diploid and subsequently undergo the meiotic process on the ME solid medium. The conjugated cells in meiosis were scraped off from the medium and resuspended in EMM liquid medium lacking nitrogen (EMM-N medium). Chromosomal DNA was stained with Hoechst 33342 as previously described (Ding *et al.*, 1998) before resuspending the cells in the medium. The cells were mounted on glass slides and those that were between 10 and 16 μm in the cell length were examined for microtubule dynamics with the use of the optical sectioning microscope system described below. We chose conjugated cells with a relatively straight shape to facilitate analysis, because irregular-shaped cells probably complicate the interpretation of microtubule dynamics and nuclear movements.

Optical Sectioning Microscopy and Computer Image Procession

The computer-operated microscope system used in this study was previously described (Haraguchi *et al.*, 1999). Cells expressing GFP-labeled microtubules or GFP-tagged DHCs were observed with the use of a 60×/1.4 numerical aperture Plan Apo oil immersion objective (Olympus, Tokyo, Japan). GFP-labeled microtubule dynamics were analyzed with the use of images from 10 or 15 focal planes spaced at 0.4- or 0.2-μm intervals, respectively. The exposure times used (0.2–0.6 s) did not cause observable alterations in nuclear movement. The time points were collected continuously, such that the time between each time point was limited only by acquisition time required for each data point. Therefore, the time required for recording each set of images was used as the time interval between the projections. Images were processed by deconvolution and then combined to form a two-dimensional projection (Hiraoka *et al.*, 1989). The position of the microtubule focus was regarded as the location of the SPB. We regarded microtubules with the lowest intensity of GFP signal as single microtubules, and microtubule length was measured by tracing those microtubules on each projection from the center point of the focus to the distal ends. GFP-tagged DHC was analyzed from images collected at 8 or 15 focal planes spaced at 0.5- or 0.2-μm intervals, respectively, with 0.2-s exposures and processed like those of GFP-labeled microtubules.

Laser Photobleaching of GFP-labeled Microtubules

Cells prepared as described above were examined with the use of an Olympus IX70 inverted microscope and a 100×/1.4 numerical aperture Plan Apo oil immersion objective lens (Olympus). A 10-mW single-line (488 nm) argon-ion-laser (model 532-15BS; Omnichrome, Chino, CA) was used to both visualize and photobleach GFP-labeled microtubules by splitting the laser beam into an observation and a photobleaching beam. For observing the GFP-labeled microtubules, the laser beam was focused at the back-focal plane of the objective lens and the intensity adjusted by means of attenuators placed in the beam. For the photobleaching of GFP-labeled microtubules, the laser beam was expanded and collimated. The collimated beam entered the back aperture of the microscope objective lens and was brought to a focus at the specimen.

The illuminated area used for the photobleaching had an approximate diameter of 2 μm and the cell was exposed to the laser beam for 2 s. The power density given at the spot was $\sim 3 \times 10^7$ W/m^2, which was ~650-fold greater than that used to observe GFP-labeled microtubules. Images of GFP-labeled microtubules were monitored with the use of a digital image processor (Argus-20; Hamamatsu Photonics, Hamamatsu, Japan) and recorded on videotape. Recorded images were analyzed for changes in the length of GFP-labeled microtubules with the use of the Scion Image program (available on the Internet at http://www.scioncorp.com/). Only images of microtubules from a single focal plane were analyzed after photobleaching.

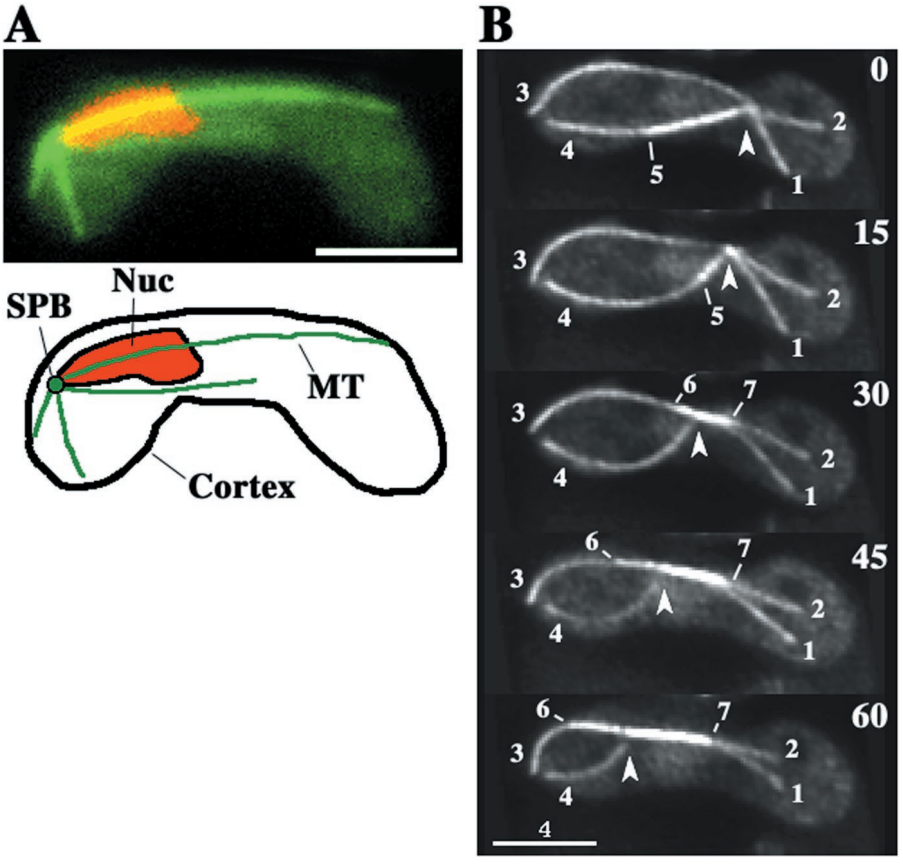

Figure 1. Microtubule organization during nuclear oscillation in wild-type cells. (A) Wild-type cell (strain CRL152) expressing GFP-tagged alpha-tubulin in the nuclear oscillation stage. The cell was observed in a single focal plane. GFP-labeled microtubules and chromosomal DNA stained with Hoechst 33342 are shown in green and red, respectively. Bar, is 4 μm. (B) Projections from optical sectioning microscopy of a single cell in the nuclear oscillation stage. Each projection was constructed from images of 15 different focal planes (see MATERIALS AND METHODS). Barbed arrowheads indicate the position of a microtubule focus where the SPB is located. Large numbers indicate time in seconds. Small numbers identify individual microtubules. Bar, 4 μm.

RESULTS

Microtubule Organization during Nuclear Oscillation

During nuclear oscillation, microtubules labeled with GFP-tagged alpha2-tubulin generally radiate from the SPB at the leading end of the nucleus (Figure 1A). Because the microtubules exist in three-dimensional space, we used optical sectioning microscopy to follow their dynamic changes. Figure 1B shows the typical behavior of GFP-labeled microtubules during nuclear oscillation observed in our system. Microtubules radiated from a single point. The cell cortex was shown by the edge of the diffused GFP signal in the cytoplasm, and the radial microtubules contact it either by lateral association (Figure 1B, microtubule 3) or via interaction at their tips (Figure 1B, microtubule 1). Some of the radial microtubules formed bundles as shown by the more intense GFP signal of their portions (Figure 1B, microtubule 5–7). As the radial microtubules changed their lengths and spatial arrangement, the SPB moved along the longitudinal axis of the cell (Figure 1B, arrowheads).

SPB Migrations during Nuclear Oscillation

To understand the relationship between nuclear migrations and microtubule dynamics, we first characterized migration of the SPB. The SPB oscillated between the two ends of the cell (Figure 2A), as previously reported (Ding *et al.*, 1998). We now distinguish the SPB motility as occurring in two phases (Figure 2B). In phase I, the SPB migrated continuously from one-half of the cell to the other covering a distance of >5 μm (Figure 2A, 30–120 and 180–405 s). The rate of this migration was variable (1.5–12 μm/min) with a mean of 4.3 ± 2.7 μm/min (n = 37). In phase II, the SPB paused or slowly wandered (<2 μm/min) a short distance (<3 μm) in one-half of the cell. Phase II was observed during reversal of the SPB movements: it generally began, when the SPB made contact with the cortex around the cell ends (Figure 2A, 120–180 s; and B), and continued until the SPB started movement toward the opposite pole, thereby starting the next phase I (Figure 2A, 30 and 180 s). Phase II persisted for 50–180 s with an average of around 100 s (n = 10).

SPB Migrations follow Forward-extending Microtubules

We next examined the relationship between SPB migrations and spatial arrangement of the radial microtubules. We found a strong correlation between the arrangement of the forward-extending microtubules and the route of SPB migrations. In 18/19 observations, SPB migrations followed forward-extending microtubules or microtubule bundles (Figure 3); the route taken by the SPB coincided with the initial arrangement of these microtubules (Figure 3A, b). The majority of phase I migrations followed a

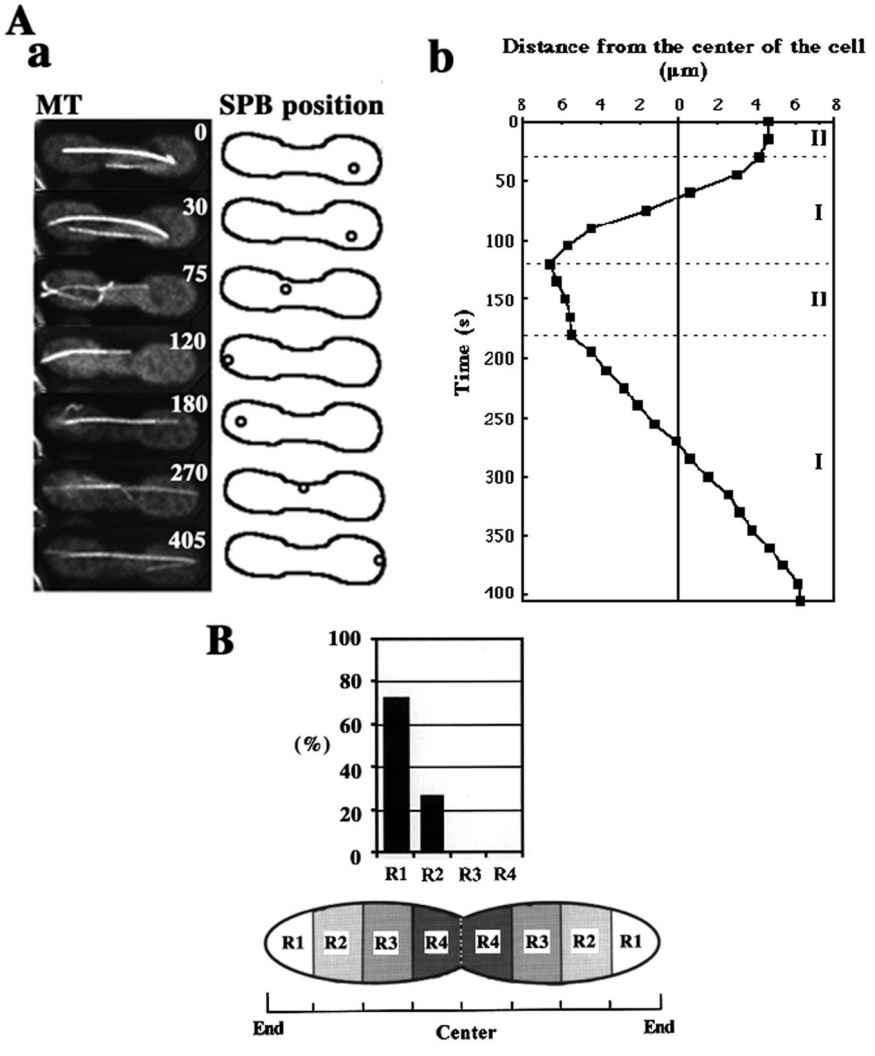

Figure 2. Two phases of SPB movement during nuclear oscillation. (A) Microtubule appearance and positions of the SPB shown by a microtubule focus during nuclear oscillation. In a, left column shows projections of a cell containing GFP-labeled microtubules, and right column shows cartoons indicating the position of the SPB. The numbers in the projections indicate the time in seconds. Circles and solid lines in the cartoons indicate the positions of the SPB and the cell cortex, respectively. In b, the position of the SPB in the same cell is shown by its distance from the equator of the cell. The position of the SPB in the left or right half of the cell is, respectively, plotted in the left or right side. The dotted lines indicate borders between phase I and phase II. (B) Position of the SPB at transitions from phase I to phase II. Eleven transitions were examined for SPB positions. Cells were equally divided into four regions along the horizontal axis (R1 to R4) as shown in a cartoon. Graph indicates percentages of the SPBs in different regions at the transition.

single microtubule or a single microtubule bundle (16/18), and the remaining migrations successively followed a series of individual microtubules or microtubule bundles. Below, we refer to these microtubules as "directing microtubules."

In contrast to forward-extending microtubules, no strong correlation was noted between the spatial arrangement of rearward-extending microtubules and SPB migration. The majority of the ends of rearward-extending microtubules mapped to various positions during SPB migrations (21/24 microtubules in 19 SPB migrations; Figure 3A, c). These microtubules with unfixed ends frequently appeared to be being dragged along the cortex by the migrating SPB (Figure 3A, a, microtubule 2; and c). There were also occasions when we failed to detect any rearward-extending microtubules (Figure 3B, 0 and 26 s).

During phase II, several short microtubules were frequently in contact with the cortex near the SPB. However, the relationship between the arrangement of these microtubules and SPB movements was unclear.

Relationship between Behavior of Directing Microtubules and SPB Movement

We examined the relationship between the behavior of directing microtubules and SPB movement in greater detail. The majority of the directing microtubules were in lateral association with the cortex by curving along it (19/22 microtubules; Figure 3C, a and b). In contrast, other microtubules appeared to be in contact with the cortex at their tips (Figure 3C, c). The cortical association sites of the microtubules remained fixed in position near the cell pole in a majority of cases (~60 and ~30% of directing microtubules contact, respectively, with R1 and R2 regions shown in Figure 2C [n = 22]).

The directing microtubules generally disassembled at the cortex and shortened during SPB migrations (see below). However, some of the ends of the directing microtubules that were in a lateral association with the cortex moved forward as the SPB migrated (9/22 microtubules; Figure 3C, a), indicating that these microtubules slid along the cortex at the cortical interaction sites. The ends of other microtubules remained fixed in position (Figure 3C, b and c).

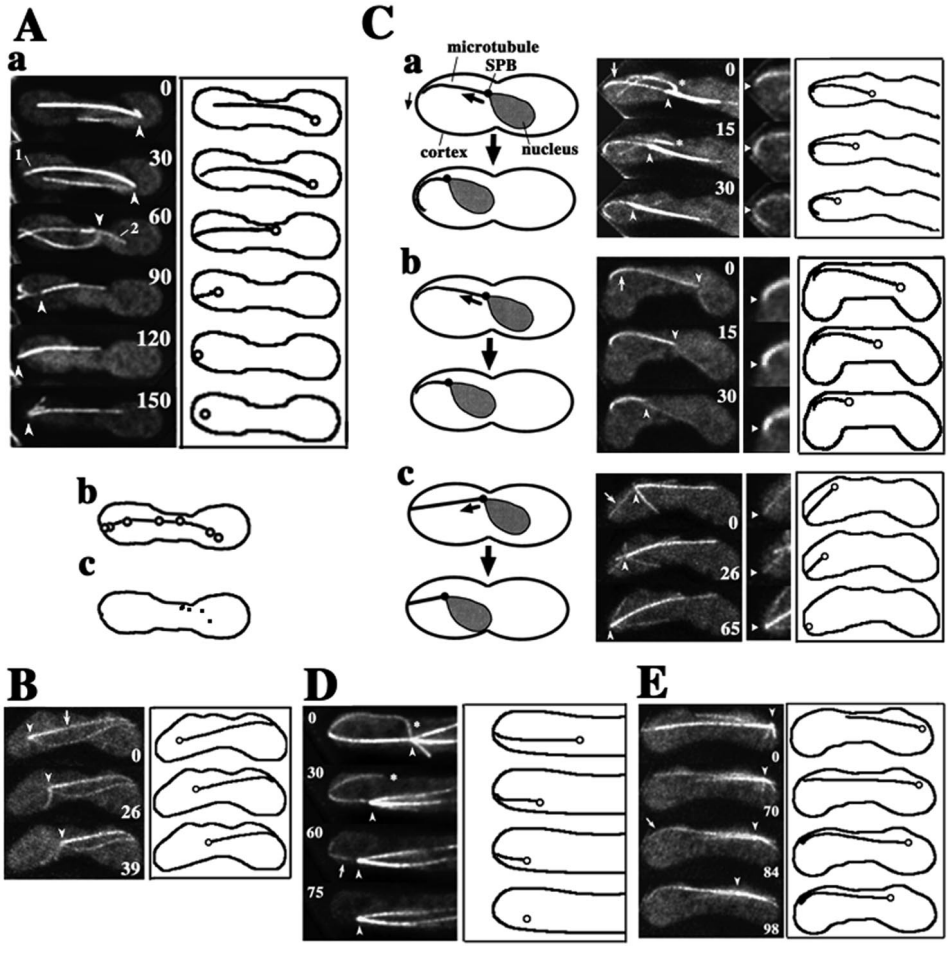

Figure 3. Relationship between the behavior of microtubules and SPB migrations. (A) Spatial arrangement of a directing microtubule and rearward-extending microtubules from the beginning of an SPB migration to its end. In a, left column indicates projections of a cell containing GFP-labeled microtubules; large and small numbers are time in seconds and microtubule numbers, respectively. The right column indicates cartoons showing the SPB (circles), directing microtubules (solid lines extending from the circles), and the cell cortex (solid outlines). In b, positions of the SPBs at 15-s intervals from 30 to 120 s superimposed on a directing microtubule (microtubule 1) at 30 s. In c, dots show positions of the end of microtubule 2 at 15-s intervals from 60 to 120 s. (B) SPB migration after a directing microtubule (arrow) in the absence of rearward-extending microtubules. (C) Interaction of directing microtubules with the cell cortex. In a, directing microtubule laterally interacts with the cortex, and its end moves along the cortex during SPB migration. In b, directing microtubule laterally interacts with the cortex with its end fixed in position. In c, directing microtubule interacts with the cortex at its end. Left cartoons are schematic diagrams of these interactions. Large arrows indicate movements of the SPB. Small arrow indicates movement of the end of a directing microtubule. Projections on the right are enlarged portions of the projections on the left. Arrows in the left projections indicate directing microtubules. Arrowheads in the right projections indicate positions of the ends of directing microtubules at time zero. Right cartoons show positions of the SPB, directing microtubules, and the cell cortex. (D) Cessation of SPB migration upon disappearance of a directing microtubule. An arrow indicates a directing microtubule, which disappears. (E) Start of SPB migration upon lateral association of a directing microtubule with the cortex. Arrow indicates cortical association of a directing microtubule. Barbed arrowheads in the projections in A to E indicate positions of microtubule foci. Asterisks in C, a and D indicate microtubules released from the SPB.

SPB migrations switched from phase I to phase II when directing microtubules disappeared by microtubule shortening: upon microtubule disappearance, the SPB paused or started wandering (11/11 migrations; Figure 3D, arrow). On the other hand, a switch from phase II to phase I took place when microtubules elongated to reach the cortex near the distal end of the cell. Once an interaction between the cortex and these microtubules was established, the SPB migrated in the direction of the microtubule extension (13/14 migrations; Figure 3E, arrow). These observations suggest that cortical interactions of forward-extending microtubules drive meiotic nuclear migrations.

Microtubule Shortening Is Induced in Front of Migrating Nucleus

It has been shown in budding yeast that some nuclear migrations are coupled with microtubule elongation or shortening (Shaw *et al.*, 1997; Maddox *et al.*, 1999; Adames and Cooper, 2000; Maddox *et al.*, 2000). We examined the relationship between the changes of microtubule length and nuclear migrations in fission yeast.

Throughout the period of nuclear oscillations, microtubule lengths changed at approximately the same rate (Figure 4A, a). The shortening rate was faster on average than the elongation rate (Figure 4B and Table 1), and these values were similar to those reported for cytoplasmic microtubules during mitotic interphase (Drummond and Cross, 2000). The elongation rates of microtubules in phase I and phase II were not significantly different (Table 1). In contrast, the shortening rate of microtubules in phase I was significantly slower than that in phase II (~0.6 times; Table 1). Microtubules frequently underwent transitions from elongation to shortening (Figure 4A, a), whereas we never saw transitions from shortening to elongation (Table 1). Periods in which microtubule length did not change were also frequently observed,

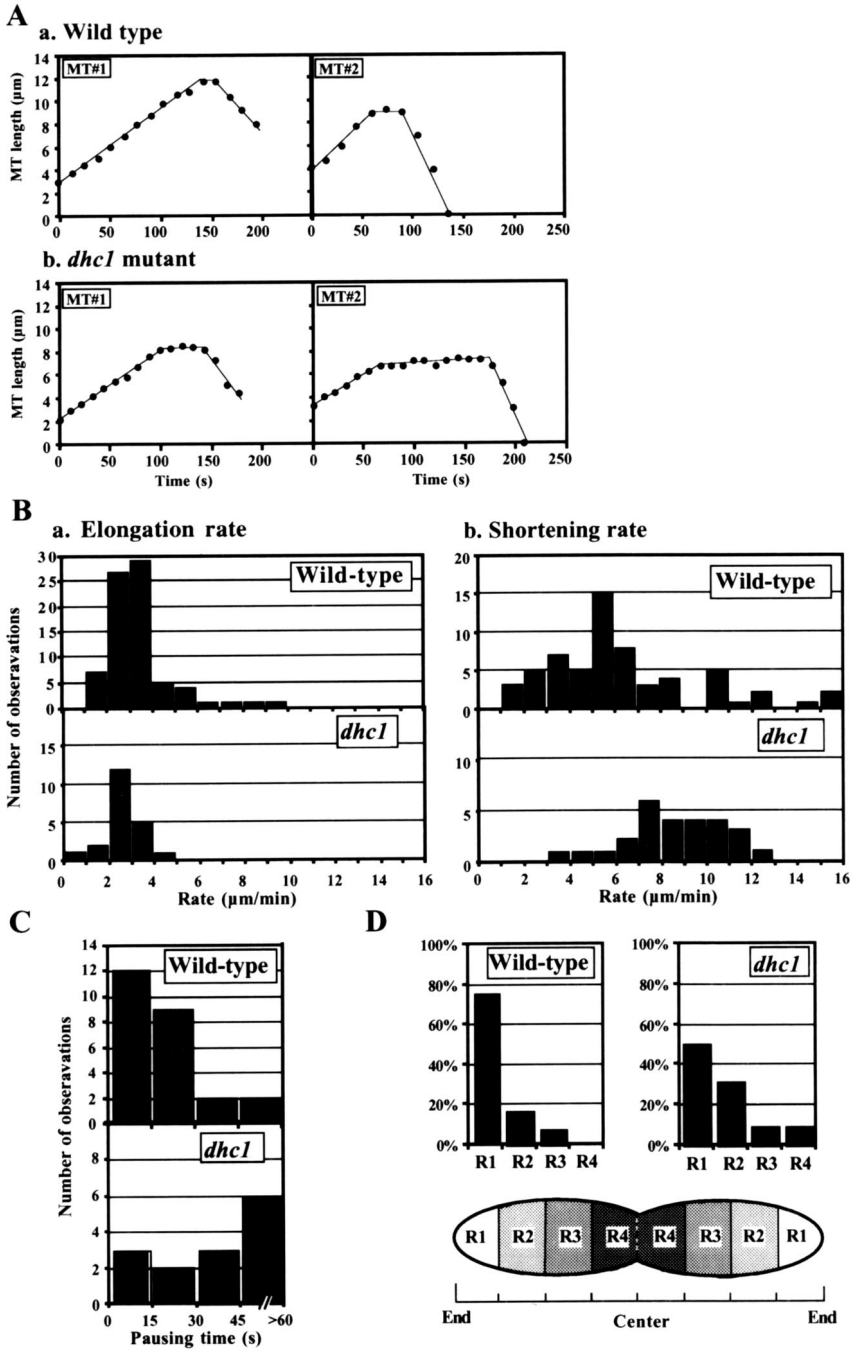

Figure 4. Dynamic properties of microtubules during the nuclear-oscillation stage in wild-type and the *dhc1*$^-$ mutant cells. (A) Plots of the microtubule length in wild-type (a) and *dhc1*$^-$ mutant (b) cells. Two representative examples (MT1 and MT2) of each strain are shown. (B) Distribution of the elongation (a) and the shortening (b) rates of wild-type (top) and the *dhc1*$^-$ mutant cells (bottom). (C) Distribution of pausing times of microtubules in wild-type (top) and the *dhc1*$^-$ mutant cells (bottom). (D) Positions of the ends of microtubules at their maximal lengths during their transitions from elongation to shortening. Graph shows percentages of the ends in different regions in wild-type (left, n = 42) and the *dhc1*$^-$ mutant (right, n = 32) cells. Cells were divided into four regions of equal size along the horizontal axis (R1–R4).

although briefly (71% [25/35 transitions]; Figure 4A, a). The duration of these static phases was mostly <30 s (21/25; Figure 4C) and ~25 s on average.

Shortening of microtubule was strongly correlated with nuclear migrations. Microtubule shortening was largely initiated in front of the migrating SPB during phase I (Figure 5A, a), and in the majority of cases, forward-extending microtubules shortened during phase I, whereas rearward-extending microtubules or phase II microtubules continually elongated (Figure 5A, b). Furthermore, the shortening of directing microtubules was largely coupled with SPB migrations. Their shortening mostly began at the same time as SPB migrations (11/15 cases; Figure 5B, a) and the shortening rates were often similar to the SPB velocities (Figure 5B, b). Directing microtubules usually disappeared upon arrival of the SPB at a cortical interaction site (Figure 3, A, a, 120 s; and C, c, 65 s). Together with the slower shortening rate in phase I, these observations indicated the presence of a mechanism

Table 1. Microtubule parameters during meiotic prophase
Rates are mean ± SD. In *dhc1*$^+$ cells, when microtubules were observed over two phases, their rates were examined in each phase.

Genotype	Parameters		No. of microtubules[a]
dhc1$^+$	Elongation rate (μm min^{-1})	3.4 ± 1.4[b]	76
	Phase I	3.5 ± 1.4[c]	60
	Phase II	3.2 ± 1.4[c]	19
	Shortening rate (μm min^{-1})	6.4 ± 3.4[d]	61
	Phase I	3.9 ± 6.2[e]	48
	Phase II	6.2 ± 3.1[e]	15
	Maximum length (μm)	8.2 ± 3.6[f]	52
	Transition frequency (s^{-1})		
	Elongation to shortening	0.006[g]	69
	Shortening to elongation	0[h]	44
dhc1-d2	Elongation rate (μm min^{-1})	2.7 ± 0.8[b]	22
	Shortening rate (μm min^{-1})	8.5 ± 2.2[d]	27
	Maximum length (μm)	5.3 ± 1.9[f]	27
	Transition frequency (s^{-1})		
	Elongation to shortening	0.010[i]	25
	Shortening to elongation	0[j]	26

[a] Number of microtubules that were examined.
[b] *t* test showed significant difference between values ($P < 0.005$).
[c] *t* test showed no significant difference between values ($P > 0.01$).
[d–f] *t* test showed significant difference between values ($P < 0.001$).
[g] Forty-one transitions/6730 s of total elongation time.
[h] Zero transitions/3423 s of total shortening time.
[i] Seventeen transitions/1621 s of total elongation time.
[j] Zero transitions/889 s of total shortening time.

that induces and regulates microtubule shortening in front of the migrating nucleus.

Microtubules Are Disassembled at Cell Cortex

Microtubules change their length by the assembly or disassembly of tubulin subunits at their ends. To understand how microtubule shortening was induced and regulated in front of a migrating nucleus, we examined whether microtubule disassembly takes place at the microtubule end distal to the SPB, or at the SPB proximal end. The middle of microtubules was marked by bleaching the GFP signal with the use of a laser beam, and changes in the length of GFP-labeled microtubules were examined. During the shortening of a single or a bundle of microtubules, the length of the GFP-labeled region of the microtubules between the bleached zone and the cortex changed; and the length of the region between the SPB and the bleached zone as well as the length of the bleached zone did not change (n = 9; Figure 6A). These observations indicate that disassembly of microtubules took place at the microtubule ends distal to the SPB, but not at the proximal ends. During the course of this analysis, we also noted that during microtubule elongation, microtubule assembly took place at the distal ends, but not at the proximal ends (n = 6; Figure 6B).

When microtubules underwent transitions from elongation to shortening, most of the microtubule ends distal to the SPB were in contact with the cortical regions at the cell ends (Figure 4D). Furthermore, some of the directing microtubules underwent rapid disassembly in these cortical regions (3/18 microtubules; Figure 7A), resulting in abrupt shortening of the microtubule by more than a distance of SPB migration (Figure 7B). Occasionally, the same microtubules repeatedly underwent rapid disassembly at the same cortical region: the microtubule that underwent rapid disassembly moved forward by sliding along the cortex, and subsequently underwent rapid disassembly again at the cortical region where the previous disassembly took place (Figure 7A, arrowheads). These observations suggest the presence of a factor at the cortical regions around the cell ends that induces microtubule disassembly.

Microtubule Dynamics Is Significantly Altered in Dynein Mutant

To understand the role played by cytoplasmic dynein in the functions of astral microtubules, we examined microtubule behavior in *dhc1*$^-$ mutant cells. The microtubule arrays of the mutant cells in meiotic prophase resembled those of wild-type cells: they radiated from a single point at the SPB (Figure 8; Yamamoto *et al.*, 1999). In the mutant cells, however, the SPB did not oscillate between the cell ends and generally remained in the middle of the cell (Figure 8, A and C). SPB movements after forward-extending microtubules were never observed, whereas the SPB occasionally moved a short distance (<2 μm) at a velocity of ≤2.5 μm/min (Figure 8B). Such movements were rare, however, with just five such movements observed in eight cells after ~40 min. These small movements were accompanied by the elongation of rearward-extending microtubules whose ends remained fixed in the position on the cortex (Figure 8B, microtubule 3), suggesting that these movements were driven by a pushing force generated by elongation of rearward-extending microtubules. These observations suggested that cytoplasmic dynein is required for nuclear movements driven by forward-extending microtubules but not for those driven by rearward-extending microtubules.

In the *dhc1*$^-$ mutant cells, microtubules underwent both elongation (Figure 8A, microtubule 1, and B, microtubule 3) and shortening (Figure 8A, microtubule 2), and they often formed bundles as in wild-type cells. Photobleaching experiments showed that microtubule assembly and disassembly took place at the microtubule ends distal to the SPB.

However, microtubules failed to establish lateral interactions with the cortex, suggesting that cytoplasmic dynein is required for cortical interactions of directing microtubules. Furthermore, the dynamics of microtubule assembly and disassembly were altered in the *dhc1*$^-$ mutant: the average shortening rate was faster (~1.3 times) than in wild type, whereas the average elongation rate was slower (~0.8 times) than in wild type (Table 1). Frequency of transitions from elongation to shortening was increased in the *dhc1*$^-$ mutant cells. Consistent with the increased frequency of the transitions, the average maximum length of microtubules was significantly shorter (~0.6 times) in the *dhc1*$^-$ mutant (Table 1), although the cell size was not significantly different (average longitudinal cell lengths of wild-type and the *dhc1*$^-$ mutant cells were 13.3 ± 0.8 μm [n = 6] and13.1 ± 1.8 μm [n = 8], respectively). The population of microtubules that reached the cortical regions around the cell ends was also reduced (Figure 4D). Although growth pause at microtubule transitions from elongation to shortening was frequent as in

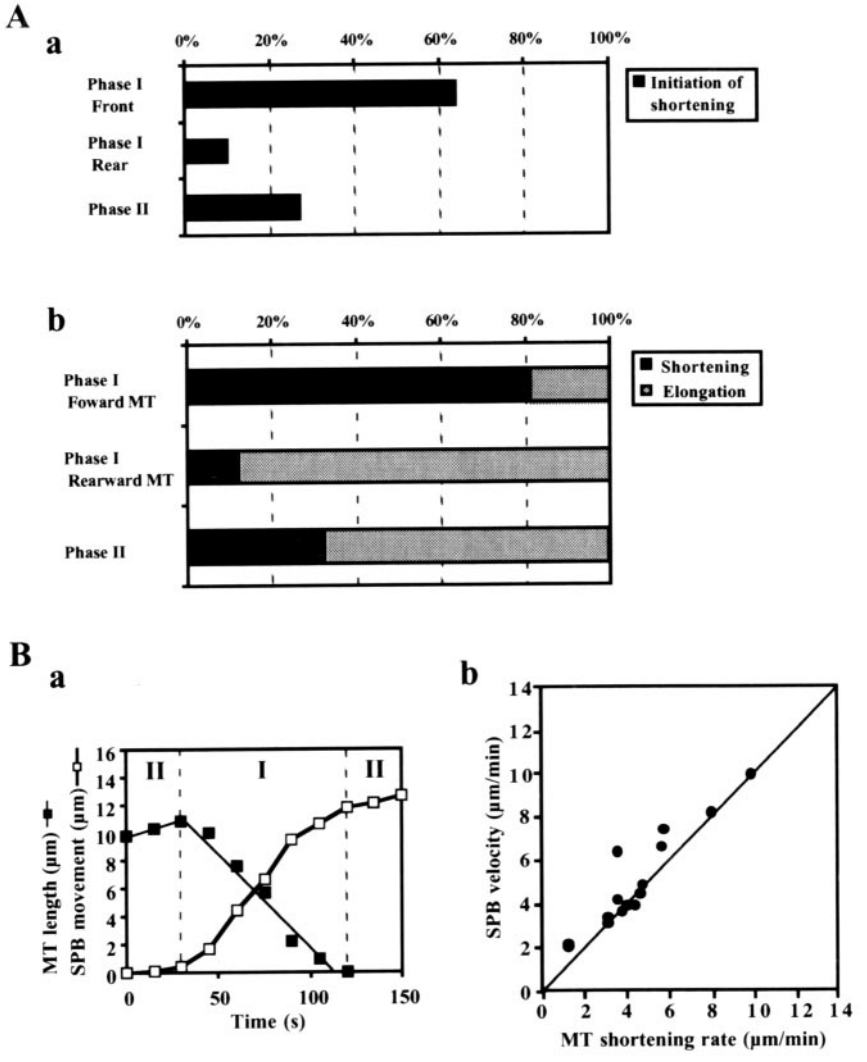

Figure 5. The relation between microtubule shortening and SPB migrations. (A) Behavior of microtubules in different phases and positions. In a, position of the microtubule ends and phase of the SPB migration were examined at the initiation of microtubule shortening and the initiation events of the microtubules were scored with the use of three different categories: the front side of the SPB in phase I (Phase I, Front), the rear side of the SPB in phase I (Phase I, Rear), and Phase II. The graph indicates percentages of each category (n = 52). In b, shortening or elongating microtubules were counted in different phases and positions relative to the SPB. Microtubules that elongated and subsequently shortened were counted as shortening. When microtubules were examined over two phases, their behaviors were counted in each phase. Black and gray bars show percentages of microtubules undergoing shortening and continuing elongation, respectively: 43 forward-extending and 42 rearward-extending microtubules in phase I and 50 microtubules in phase II were examined. (B) Shortening of directing microtubules coupled with SPB movement. In a, length of a directing microtubule (■) and distance of SPB movement (□) are plotted against time. Phase I and II are separated by vertical, broken lines. In b, SPB velocities are plotted against the shortening rates of directing microtubules (●). The line indicates the velocity equal to the shortening rate. The SPB velocities faster than the shortening rates were accompanied by microtubule sliding.

wild-type cells (82% [14/17 transitions]), the duration of these phases was generally twice as long (~46 s [n = 17]; Figure 4A, b; and C). The extension of these phases in the mutant was not caused by reduced microtubule interactions with the cortical regions around the cell ends where the microtubule-disassembling activity may be present (Figure 4D), because the pausing time of microtubules reaching the R1 region was still longer in *dhc1*$^{-}$ mutant than in wild type on average (~39 and ~16 s for the mutant [n = 8] and wild type [n = 20], respectively). These results indicated that dynein plays a role in the regulation of assembly and disassembly of microtubules.

Accumulation of Dynein at Cortical Interaction Sites of Directing Microtubules

Using GFP-tagged DHC (GFP-DHC), we previously found that dynein was localized at the SPB and astral microtubules (Figure 9A; also see Figure 8 in Yamamoto *et al.*, 1999). We also found that dynein frequently accumulated at the cortical site where directing microtubules met the cell's boundary (Figure 9A, small arrowhead), suggesting that dynein mediates the cortical interaction of directing microtubules. To understand the role of dynein at the cortical interaction sites of directing microtubules, we examined the dynamics of cortical accumulation of GFP-DHC in living cells with the use of time-lapse, optical sectioning microscopy. GFP-DHC localized at the SPB and microtubules was seen as a large GFP dot and lines, respectively. Consistent with the behavior of the SPB and directing microtubules, a large GFP dot moved along the path of a GFP line (Figure 9B, large arrowheads). During movements of the large GFP dot, GFP-DHC frequently accumulated at the cortical interaction site of a GFP line (13/22 movements; Figure 9B, small arrowheads). The large GFP dot eventually reached the accumulation site then paused or slowly wandered, as observed for SPB movement during phase II (Figure 9B, left column, 75 and 90 s). Alternatively, it moved toward another cortical site where GFP-DHC accumulated (Figure 9B, right column, 48–112 s). After the SPB moved away from the cortical site, the GFP-

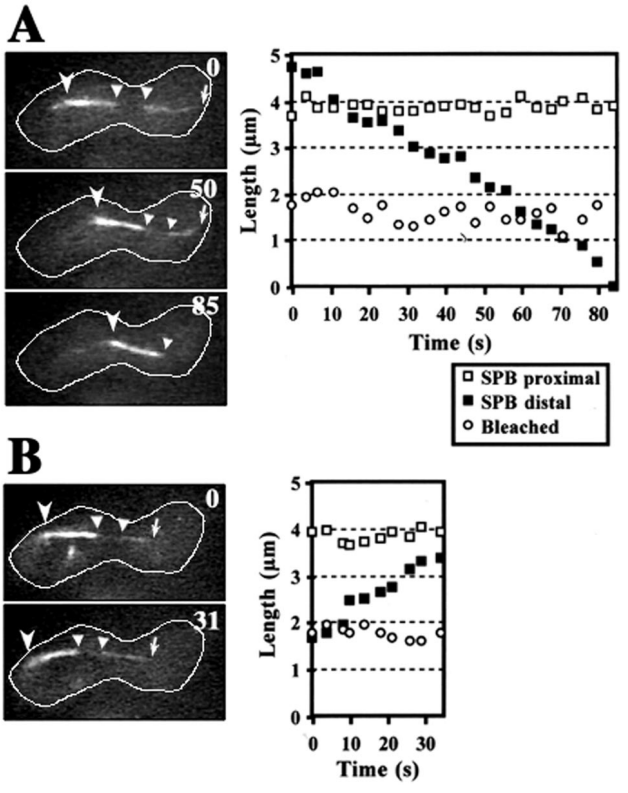

Figure 6. Photobleaching of GFP-labeled microtubules during nuclear oscillation. The GFP signal of a bundle of microtubules was photobleached in the middle and the bundle was examined at a single focal plane (see MATERIALS AND METHODS). Shortening (A) and elongation (B) of the photobleached microtubule bundle. Left photos indicate images of the photobleached microtubule bundle. Numbers indicate time in seconds. Barbed and small arrowheads indicate a microtubule focus and the bleached microtubule region, respectively. Arrows indicate the end of the microtubule bundle distal to the SPB. White lines indicate the cell cortex. Right graphs show lengths of GFP-labeled and -bleached microtubule regions versus time. Open and closed squares indicate lengths of GFP-labeled regions proximal and distal to the SPB, respectively. Open circles indicate lengths of the bleached microtubule region.

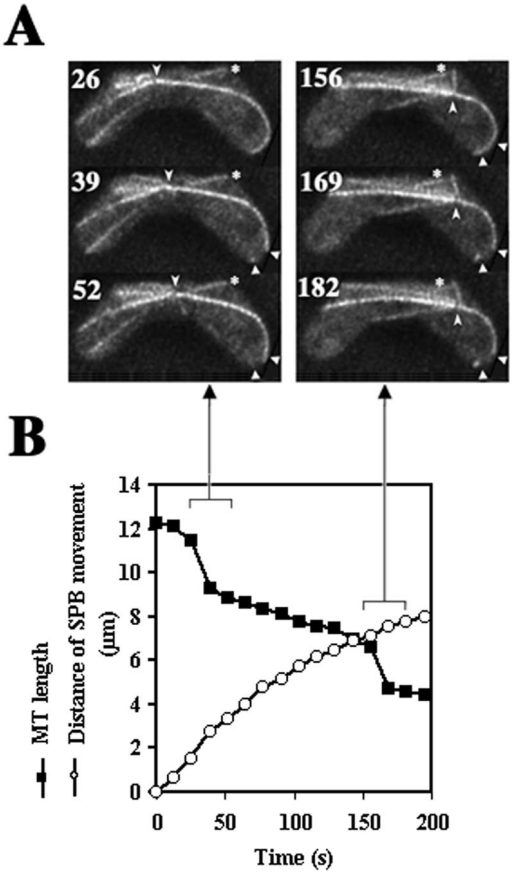

Figure 7. Rapid disassembly of microtubules at the cortex. (A) Projections of a cell containing a GFP-labeled microtubule undergoing rapid disassembly. Numbers indicate time in seconds. Barbed arrowheads indicate positions of the SPB. Small arrowheads indicate the cortical region where a directing microtubule disassembled (39 s). The disassembly at 169 s occurred at the same cortical region. Arrows indicate a directing microtubule. Asterisks indicate a microtubule that is not radiating from the SPB. (B) Changes in the length of a directing microtubule (■) and the distance of SPB movement (○) versus time. Arrows indicate projections showing a sharp decrease in the microtubule length.

DHC accumulated at the cortex was not observed (Figure 9B, arrows). These observations strongly support the idea that cytoplasmic dynein mediates cortical interaction of directing microtubules.

DISCUSSION

Nuclear Migrations Are Driven by Forward-extending Microtubules

In this study, we have examined the behavior of microtubules in relation to nuclear migration during meiotic prophase in fission yeast. Several lines of evidence suggest that a major force driving nuclear migrations is a pulling force generated by cortical interaction of microtubules. First, SPB migrations follow forward-extending microtubules, which we refer to as "directing microtubules." Second, SPB migrations started when the directing microtubules established interactions with the cell cortex. Third, SPB migrations ceased when the directing microtubules disappeared. Fourth, in the dynein-mutant cells where nuclear oscillation is abolished, we never saw SPB migrations after forward-extending microtubules. Finally, rearward-extending microtubules were not essential for SPB migrations.

It has been proposed previously that a pushing force generated by elongation of microtubules drives nuclear migrations based on the observation that rearward-extending microtubules elongate during nuclear migration with their ends fixed in position (Ding *et al.*, 1998). However, our analysis with the use of high-resolution microscopy showed that rearward-extending microtubules elongated, whereas their ends were rarely fixed in position in wild-type cells. We therefore speculate that the contribution from microtubule elongation is small.

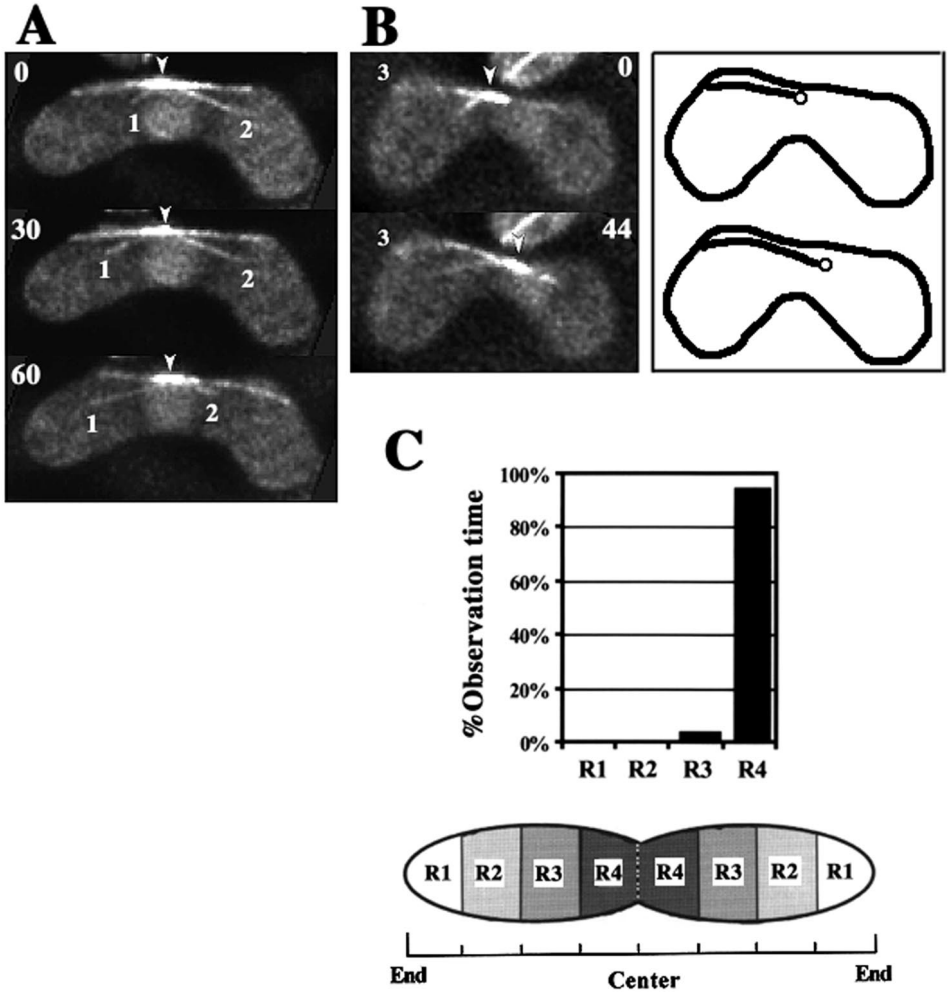

Figure 8. Microtubule behavior and SPB position in the *dhc1*$^-$ mutant cells. (A and B) Projections of the mutant cells containing GFP-labeled microtubules. Cartoons on the right in B show the SPB (circles), microtubule 3 (solid lines extending from the circles), and the cell cortex (solid lines). Barbed arrowheads indicate positions of a microtubule focus. Large numbers indicate time in seconds. Small numbers indicate microtubule numbers. (C) Frequency of the positions of the SPB within the cell. Positions of the SPB were examined in eight independent cells with total observation time of 42 min and 46 s.

We propose that a major force driving nuclear migrations is a pulling force. This force might be generated by movement of the SPB along the directing microtubules. However, this seems unlikely, because our photobleaching analysis showed that the SPB remains at the ends of the microtubules where their disassembly or assembly does not take place. Rather, we speculate that the force is generated by the sliding of directing microtubules along the cortex, given the coincidence of directing microtubule sliding on the cortex with SPB migrations. Similar models have been proposed for the generation of forces driving nuclear migrations in other organisms (Koonce *et al.*, 1999; Adames and Cooper, 2000). Disassembly of directing microtubules at the cortex may also contribute to force generation, because directing microtubules were shortened in a manner that was largely coupled with SPB migrations. However, because there are occasions when microtubule shortening is uncoupled with SPB migrations (Figures 5B, b; and 7B), microtubule disassembly is not essential for SPB migrations. It is likely that the shortening of directing microtubules is essential for changes in the direction of SPB migrations, because the ultimate disappearance of the microtubules through shortening results in the termination of SPB migration. This would allow another directing microtubule to drive SPB migration in the reversed direction.

Two lines of evidence suggest that directing microtubules are shortened by microtubule-disassembling factors present at the cortical regions around the cell ends. First, directing microtubules shortened by disassembly at the ends distal to the SPB, and these microtubule ends appeared to be attached to the cortical regions during their shortening. Second, the directing microtubules occasionally disassembled rapidly at the cortical regions. It is likely that these disassembling factors also induce shortening of other microtubules in front of the migrating nucleus.

Roles of Dynein in Nuclear Oscillation

Cytoplasmic dynein is probably required for nuclear migrations driven by forward-extending microtubules, because these migrations were absent in *dhc1*$^-$ mutant. Two lines of evidence suggest that dynein participates in the cortical interactions of directing microtubules. First, DHC frequently accumulates at the cortical site where directing microtubules interact with the cortex (Figure 9; also see Figure 8 in Yamamoto *et al.*, 1999). Second, directing microtubules

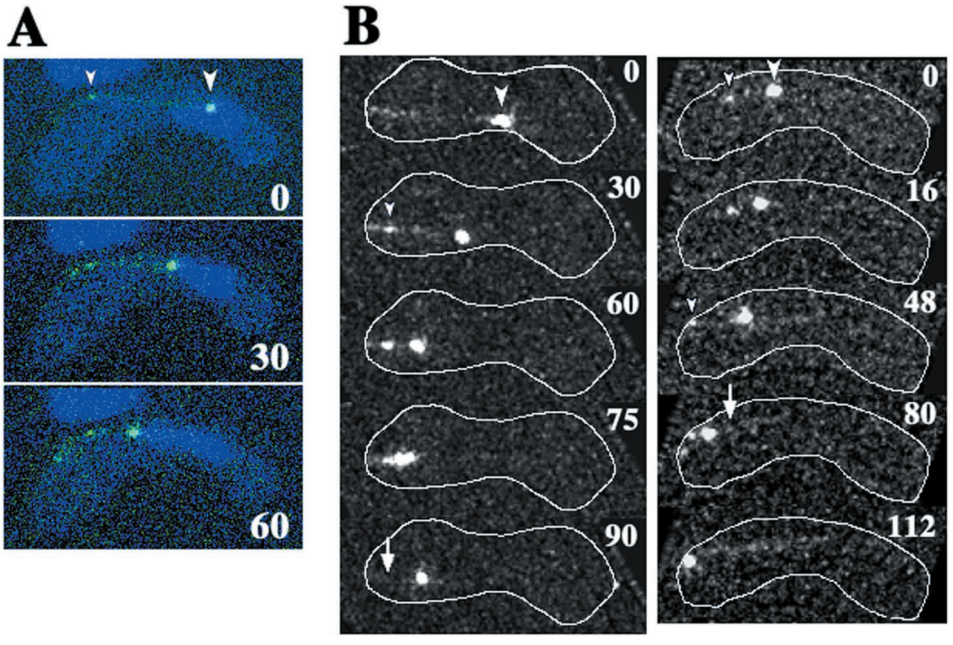

Figure 9. Dynamics of GFP-tagged DHC in living meiotic cells. (A) Time-lapse series of a meiotic cell expressing GFP-DHC (green) and stained for DNA (blue) at a single focal plane. (B) Projections of meiotic cells expressing GFP-DHC. Each projection was constructed from images of a single cell at 15 (left column) or 8 (right column) different focal planes. Each column shows projections of a single cell. White lines indicate the cell cortex. Large arrowheads indicate large GFP dots, which are located at the leading end of the moving nucleus. Small arrowheads indicate small GFP dots located at the site where a GFP line contacts with the cell cortex. In B, cortical positions of some of the small GFP dots are obscured by the projection. Arrows indicate the sites where the small GFP dots disappeared. Numbers indicate times in seconds.

mostly interacted laterally with the cortex in wild-type cells, but lateral cortical association of microtubules was never seen in dynein-mutant cells. Considering curving of directing microtubules along the cortex, it is likely that dynein establishes attachment of microtubules to the cortex at multiple sites.

We also speculate that cytoplasmic dynein participates directly in force generation. It is likely that astral microtubules are oriented with the minus ends proximal to the SPB and that dynein moves toward the minus in *S. pombe* as described in other organisms (Euteneuer and McIntosh, 1981; McIntosh and Euteneuer, 1984; Toriyama *et al.*, 1988; Yamamoto *et al.*, 1990; reviewed by Holzbaur and Vallee, 1994). Cortical dynein may drive the sliding of directing microtubules along the cortex by moving toward the minus ends of the microtubules. If the dynein is tethered to the cortex, such a motion would generate a pulling force on the SPB. A similar model has been proposed for nuclear migration into the bud neck during mitotic anaphase in budding yeast (Carminati and Stearns, 1997; Adames and Cooper, 2000). However, cortical accumulation of dynein has not been observed in budding yeast (Shaw *et al.*, 1997).

At present, the molecular basis for the accumulation of DHC at the cortex remains unknown. It may be mediated by a cortical factor(s) that interacts with DHC and activates it, like the dynactin complex in other organisms (reviewed by Karki and Holzbaur, 1999). In this model, when the microtubule reaches the cortical regions, the anchoring factors interact with the microtubule-associated DHC and activate their motile activity. As the microtubule is pulled in by the anchored DHC, microtubule-associated DHCs may accumulate at the cortex by interacting with the anchoring factors. The SPB may inactivate these anchoring factors and release the DHC from the cortex, because DHC disappears from the cortex after the SPB reaches the sites where it has accumulated (Figure 9; also see Figure 8 in Yamamoto *et al.*, 1999).

The localization of DHC at the SPB has led to the proposition that dynein generates a pushing force by moving on rearward-extending microtubules at the SPB (Yamamoto *et al.*, 1999; Yamamoto and Hiraoka, 2001). Two lines of evidence now argue against this model. First, this model assumes that microtubules elongate by assembly at the ends proximal to the SPB for continuation of DHC movement. However, microtubule assembly was not detected at the proximal ends. Second, rearward-extending microtubules appeared to generate a pushing force and drive short nuclear movements in the *dhc1*$^-$ mutant. Therefore, we consider it unlikely that DHC generates a pushing force at the SPB. Further studies will be required to establish the role (if any) of the SPB-associated DHC.

The altered microtubule assembly and disassembly dynamics in *dhc1*$^-$ mutant indicated that cytoplasmic dynein plays an additional role in regulating microtubule dynamics in fission yeast. This function may be essential for the shortening of directing microtubules that is largely coupled with SPB migration. Cytoplasmic dynein may directly regulate microtubule assembly and disassembly at the ends distal to the SPB. Such a role would be similar to that established for Kar3p, which is a budding yeast kinesin-related microtubule motor enzyme that directly promotes disassembly of microtubules at their minus ends (Endow *et al.*, 1994; Saunders *et al.*, 1997). However, assuming that dynein establishes mechanical attachments of microtubules to the cortex and that a microtubule-disassembling factor(s) is present at the cortex, we rather speculate that dynein induces microtubule shortening by recruiting the microtubule ends to the cortical disassembling factors or by activating the factors. We also speculate that dynein facilitates microtubule elongation along the cortex by driving microtubule sliding on the cortex. In this model, microtubule pulling and microtubule disassembly is not necessarily coupled one to one: the mechanical attachment site may pull in the microtubule with-

out disassembling the microtubule, whereas the cortical disassembling factors may disassemble microtubule polymer that is extending beyond the attachment site without affecting microtubule pulling. Therefore, this model can also explain the cases in which microtubule shortening is uncoupled with SPB migrations. The regulation of microtubule dynamics may be one of the conserved activities of cytoplasmic dynein in eukaryotic cells, because dynein also affects the dynamics of astral microtubules in other organisms (Carminati and Stearns, 1997; Koonce *et al.*, 1999; Adames and Cooper, 2000; Han *et al.*, 2001). To understand the mechanism of the dynein-dependent regulation of microtubule dynamics in other organisms, it may be important to focus on cortical interaction of microtubules.

Model for Meiotic Nuclear Oscillation in Fission Yeast

Based on our observations, we propose the model for meiotic nuclear oscillation shown in Figure 10. Astral microtubules are oriented with the minus ends proximal to the SPB and dynein is localized on both the microtubules and the SPB. Dynein-anchoring factors and microtubule-disassembling factors are present at the cortical regions around the cell ends (Figure 10A). The anchoring factors on the cortical region proximal to the SPB are inactive or absent. When a microtubule(s) elongates and reaches the cortical region on the opposite half of the cell, microtubule-associated dynein contacts the cortical anchoring factor and the cortical interaction of the microtubule becomes established (Figure 10B). On anchoring, dynein starts movement along the microtubule toward the minus end and generates a pulling force (Figure 10B, small arrows). Dynein also induces microtubule shortening by recruiting the microtubule ends to the disassembling factor or activating the factor (Figure 10B, dots) and the microtubule disassembly contributes further to the pulling force. The directing microtubule shortens and eventually disappears upon arrival of the SPB at its cortical interaction site, resulting in cessation of nuclear migration (Figure 10D). The SPB inactivates the anchoring factors and dynein is released from the cortex. Meanwhile, at the other end of the cell, the cortical region accumulates active anchoring factors (Figure 10C, left side). When another microtubule reaches the cortical region around the opposite pole of the cell, the events that drive nuclear migration are repeated, and the nucleus migrates back to the opposite pole.

It seems that dynein-dependent nuclear or spindle migrations in many eukaryotic cells are driven by similar mechanisms. Understanding the mechanism of meiotic nuclear oscillations in fission yeast will probably make a significant contribution to our understanding of the basic principles of nuclear or spindle migration in eukaryotes in general.

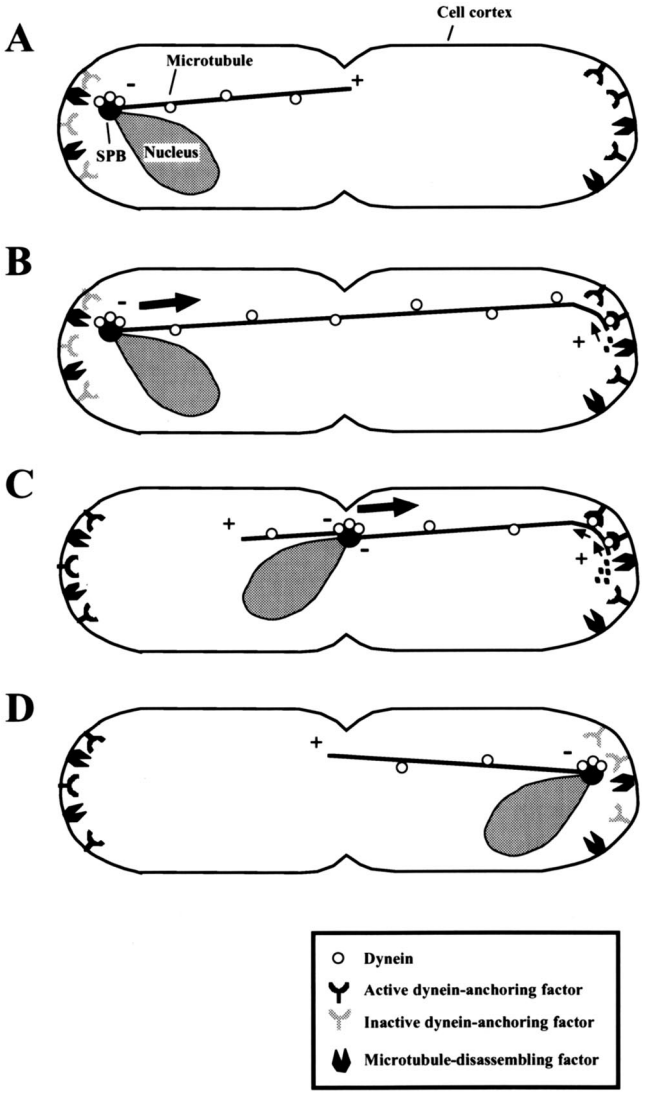

Figure 10. Model for meiotic nuclear oscillation in fission yeast. (A) Astral microtubules are oriented with their minus ends (−) proximal to the SPB (a closed circle). The dynein-anchoring factors and microtubule-disassembling factors are located at the cortical regions around the cell ends and the anchoring factors on the cortical region proximal to the SPB are inactive. (B) Astral microtubules reach the polar cortical regions and cytoplasmic dynein (open circles) localized on the microtubule (a solid line) becomes anchored to the cortex by the anchoring factor. The anchored dynein generates a pulling force on the SPB by moving along the microtubule toward the minus end (small arrows) and promoting microtubule disassembly (dots). The pulling force drives nuclear migration toward the cortex (large arrows). (C) As the nucleus approaches the cortex, the microtubule is shortened and the active dynein-anchoring factors accumulate at the cortical region (dynein-anchoring factors on the left). (D) On arrival of the SPB at the microtubule interaction site, the microtubule becomes completely disassembled and the SPB pauses. The SPB inactivates the dynein anchoring factors localized at and around the cortical interaction site of the directing microtubule and releases dynein from the cortex. +, plus ends of microtubules; −, the minus ends of microtubules.

ACKNOWLEDGMENTS

We thank Drs. D.-Q. Ding, H. Masuda, K. Okazaki, O. Niwa, I. Hagan, and R. West for critically reading the manuscript and many helpful comments to improve it. We thank M. Kikumoto for assisting analysis of images of photobleached microtubules. This work was supported by grants from the Japan Science and Technology Corporation (CREST Research Project) and the Human Frontier Science Program to Y.H.

REFERENCES

Adames, N.R., and Cooper, J.A. (2000). Microtubule interactions with the cell cortex causing nuclear movements in *Saccharomyces cerevisiae.* J. Cell Biol. *149*, 863–874.

Carminati, J.L., and Stearns, T. (1997). Microtubules orient the mitotic spindle in yeast through dynein-dependent interactions with the cell cortex. J. Cell Biol. *138*, 629–641.

Chikashige, Y., Ding, D.-Q., Funabiki, H., Haraguchi, T., Mashiko, S., Yanagida, M., and Hiraoka, Y. (1994). Telomere-led premeiotic chromosome movement in fission yeast. Science *264*, 270–273.

Ding, D.-Q., Chikashige, Y., Haraguchi, T., and Hiraoka, Y. (1998). Oscillatory nuclear movement in fission yeast meiotic prophase is driven by astral microtubules, as revealed by continuous observation of chromosomes and microtubules in living cells. J. Cell Sci. *111*, 701–712.

Drummond, D.R., and Cross, R.A. (2000). Dynamics of interphase microtubules in *Schizosaccharomyces pombe.* Curr. Biol. *10*, 766–775.

Endow, S.A., Kang, S.J., Satterwhite, L.L., Rose, M.D., Skeen, V.P., and Salmon, E.D. (1994). Yeast Kar3 is a minus-end microtubule motor protein that destabilizes microtubules preferentially at the minus ends. EMBO J. *13*, 2708–2713.

Eshel, D., Urrestarazu, L.A., Vissers, S., Jauniaux, J.-C., van Vliet-Reedijk, J.C., Planta, R.J., and Gibbons, I.R. (1993). Cytoplasmic dynein is required for normal nuclear segregation in yeast. Proc. Natl. Acad. Sci. USA *90*, 11172–11176.

Euteneuer, U., and McIntosh, J.R. (1981). Polarity of some motility-related microtubules. Proc. Natl. Acad. Sci. USA *78*, 372–345.

Gönczy, P., Pichler, S., Kirkham, M., and Hyman, A.A. (1999). Cytoplasmic dynein is required for distinct aspects of MTOC positioning, including centrosome separation, in the one cell stage *Caenorhabditis elegans* embryo. J. Cell Biol. *147*, 135–150.

Han, G., Liu, B., Zhang, J., Zuo, W., Morris, N.R., and Xiang, X. (2001). The *Aspergillus* cytoplasmic dynein heavy chain and NUDF localize to microtubule ends and affect microtubule dynamics. Curr. Biol. *11*, 719–724.

Haraguchi, T., Ding, D.-Q., Yamamoto, A., Kaneda, T., Koujin, T., and Hiraoka, Y. (1999). Multi-color fluorescence imaging of chromosomes and microtubules in living cells. Cell Struct. Funct. *24*, 291–298.

Hiraoka, Y. (1998). Meiotic telomeres: a matchmaker for homologous chromosomes. Genes Cells *3*, 405–413.

Hiraoka, Y., Minden, J.S., Swedlow, J.R., Sedat, J.W., and Agard, D.A. (1989). Focal points for chromosome condensation and decondensation revealed by three-dimensional *in vivo* time-lapse microscopy. Nature *342*, 293–296.

Holzbaur, E.L.F., and Vallee, R.B. (1994). Dyneins: molecular structure and cellular function. Annu. Rev. Cell Biol. *10*, 339–372.

Hymann, A.A. (1989). Centrosome movement in the early divisions of *Caenorhabditis elegans.* J. Cell Biol. *109*, 1185–1193.

Hyman, A.A., and White, J.G. (1987). Determination of cell division axes in the early embryogenesis of *Caenorhabditis elegans.* J. Cell Biol. *105*, 2123–2135.

Inoue, S., Turgeon, B.G., Yorder, O.C., and Aist, J.R. (1998). Role of fungal dynein in hyphal growth, microtubule organization, spindle pole body motility and nuclear migration. J. Cell Sci. *111*, 1555–1566.

Karki, S., and Holzbaur, E.L.F. (1999). Cytoplasmic dynien and dynactin in cell division and intracellular transport. Curr. Opin. Cell Biol. *11*, 45–53.

Kohli, J. (1994). Telomeres lead chromosome movement. Curr. Biol. *4*, 724–727.

Koonce, M.P., Köhler, J., Neujahr, R., Schwartz, J.-M., Tikhonenko, I., and Gerisch, G. (1999). Dynein motor regulation stabilizes interphase microtubule arrays and determines centrosome position. EMBO J. *18*, 6786–6792.

Li, Y., Yeh, E., Hays, T., and Bloom, K. (1993). Disruption of mitotic spindle orientation in a yeast dynein mutant. Proc. Natl. Acad. Sci. USA *90*, 10096–10100.

Maddox, P.S., Bloom, K.S., and Salmon, E.D. (2000). The polarity and dynamics of microtubule assembly in the budding yeast *Saccharomyces cerevisiae.* Nat. Cell Biol. *2*, 36–41.

Maddox, P., Chin, E., Mallavarapu, A., Yeh, E., Salmon, E.D., and Bloom, K. (1999). Microtubule dynamics from mating through the first zygotic division in the budding yeast *Saccharomyces cerevisiae.* J. Cell Biol. *144*, 977–987.

Maundrell, K. (1993). Thiamine-repressible expression vectors pREP and pRIP for fission yeast. Gene *123*, 127–130.

McIntosh, J.R., and Euteneuer, U. (1984). Tubulin hooks as probes for microtubule polarity: an analysis of the method and an evaluation of data on microtubule polarity in the mitotic spindle. J. Cell Biol. *98*, 525–533.

Moreno, S., Klar, A., and Nurse, P. (1991). Molecular genetic analysis of fission yeast *Schizosaccharomyces pombe.* Methods Enzymol. *194*, 793–823.

Morris, N.R. (2000). Nuclear migration: from fungi to the mammalian brain. J. Cell Biol. *148*, 1097–1101.

Neujahr, R., Albrecht, R., Köhler, J., Matzner, M., Schwartz, J.-M., Westphal, M., and Gerisch, G. (1998). Microtubule-mediated centrosome motility and the positioning of cleavage furrows in multinucleate myosin II-null cells. J. Cell Sci. *111*, 1227–1240.

Niwa, O., Shimanuki, M., and Miki, F. (2000). Telomere-led bouquet formation facilitates homologous chromosome pairing and restricts ectopic interaction in fission yeast meiosis. EMBO J. *19*, 3831–3840.

Palmer, R.E., Sullivan, D.S., Huffaker, T., and Koshland, D. (1992). Role of astral microtubules and actin in spindle orientation and migration in the budding yeast *Saccharomyces cerevisiae*. J. Cell Biol. *119*, 583–593.

Plamann, M., Minke, P.F., Tinsley, J.H., and Bruno, K.S. (1994). Cytoplasmic dynein and actin-related protein Arp1 are required for normal nuclear distribution in filamentous fungi. J. Cell Biol. *127*, 139–149.

Reinsch, S., and Gönczy, P. (1998). Mechanisms of nuclear positioning. J. Cell Sci. *111*, 2283–2295.

Reinsch, S., and Karsenti, E. (1994). Orientation of spindle axis and distribution of plasma membrane in polarized MDCKII cells. J. Cell Biol. *126*, 1509–1526.

Saunders, W., Dornack, D., Lengyel, V., and Deng, C. (1997). The *Saccharomyces cerevisiae* kinesin-related motor Kar3p acts at preanaphase spindle poles to limit the number and length of cytoplasmic microtubules. J. Cell Biol. *137*, 417–431.

Shaw, S.L., Yeh, E., Maddox, P., Salmon, E.D., and Bloom, K. (1997). Astral microtubule dynamics in yeast: a microtubule-based search-

ing mechanisms for spindle orientation and nuclear migration into the bud. J. Cell Biol. *139*, 985–994.

Svoboda, A., Bähler, J., and Kohli, J. (1995). Microtubule-driven nuclear movements and linear elements as meiosis-specific characteristics of the fission yeasts *Schizosaccharomyces versatilis* and *Schizosaccharomyces pombe.* Chromosoma *104*, 203–214.

Toriyama, M., Ohta, K., Endo, S., and Sakai, H. (1988). 51-kd protein, a component of microtubule-organizing granules in the mitotic apparatus involved in aster formation in vitro. Cell Motil. Cytoskeleton *9*, 117–128.

Xiang, X., Beckwith, S.M., and Morris, N.R. (1994). Cytoplasmic dynein is involved in nuclear migration in *Aspergillus nidulans.* Proc. Natl. Acad. Sci. USA *91,* 2100–2104.

Xiang, x., G. Han, D.A. Winkelmann, W. Zuo, and N.R. Morris. (2000). Dynamics of cytoplasmic dynein in living cells and the effect of a mutation in the dynactin complex actin-related protein Arp1. Curr. Biol. *10*, 603–606.

Xiang, X., Roghi, C., and Morris, N.R. (1995). Characterization and localization of the cytoplasmic dynein heavy chain in *Aspergillus nidulans.* Proc. Natl. Acad. Sci. USA *92*, 9890–9894.

Yamamoto, A., and Hiraoka, Y. (2001). How do meiotic chromosomes meet their homologous partners?: lessons from fission yeast. BioEssays *23*, 526–533.

Yamamoto, A., Nagai, K., Yamasaki, M., and Matsuhashi, M. (1990). Solubilization of aster-forming proteins from yeast: possible constituents of spindle pole body and reconstitution of asters *in vitro.* Cell Struct. Funct. *15*, 221–228.

Yamamoto, A., West, R.R., McIntosh, J.R., and Hiraoka, Y. (1999). A cytoplasmic dynein heavy chain is required for oscillatory nuclear movement of meiotic prophase and efficient meiotic recombination in fission yeast. J. Cell Biol. *145*, 1233–1249.

Yeh, E., Skibbens, R.V., Cheng, J.W., Salmon, E.D., and Bloom, K. (1995). Spindle dynamics and cell cycle regulation of dynein in the budding yeast *Saccharomyces cerevisiae*. J. Cell Biol. 687–700.